JOC*Note*

pubs.acs.org/joc

Synthesis of Heteroatom Substituted Naphthoporphyrazine Derivatives with Near-Infrared Absorption and Emission

Evan R. Trivedi,[†] Sangwan Lee,[†] Hong Zong,[†] Carl M. Blumenfeld,[†] Anthony G. M. Barrett,[‡] and Brian M. Hoffman*,[†]

[†]*Department of Chemistry, Northwestern University, Evanston, Illinois 60208, and* [‡]*Department of Chemistry, Imperial College of Science, Technology and Medicine, South Kensington, London, United Kingdom*

bmh@northwestern.edu

Received December 22, 2009

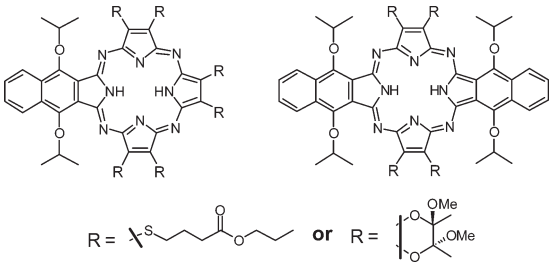

In an effort to develop effective new optical contrast agents, we report the synthesis of porphyrazines (pzs) of the form $H_2[pz(A_{4-n};C_n)]$, $n = 1$, and 2 (*trans*-), where "A" represents peripheral heteroatom (S- and O-) R-groups and "C" is a fused, β,β'-diisopropyloxynaphtho group. The sulfide appended *trans*-$H_2[pz(A_2;C_2)]$ pz (**7**) has the longest wavelength absorption, ~874 nm ($\log \varepsilon = 4.53$), and S_1 fluorescence at ~927 nm, wavelengths within the window of maximum tissue penetration. Emission from the oxygen-atom appended naphtho-pzs (**8**, **9**) has been observed within carcinoma cells, confirming cellular uptake and their potential use as optical agents.

Tetrapyrrolic macrocycles have been examined for their favorable optical properties in applications including liquid crystals,[1,2] nonlinear optical materials,[3] and biomedical photosensitizers.[4,5] Porphyrazines (pzs) are synthetically flexible macrocycles whose optical properties can be readily tuned by design, through functionalization of the aromatic core,[6] thereby customizing them for nanomaterials, photodynamic therapy (PDT), or biomedical optical imaging.[7]

Here we report the synthesis, characterization, and optical properties on a series of heteroatom functionalized naphtho-pzs of the form $H_2[pz(A_{4-n};C_n)]$ (Scheme 1), $n = 1$, and 2 (*trans*-), where "A" denotes a heteroatom substituted moiety and "C" is a fused, β,β'-diisopropyloxynaphtho group, representing a new class of compounds for use as both functional nanomaterials and optical imaging agents for cancer diagnosis. While symmetrically substituted naphthalocyanines are well studied, reports on mixed naphthophthalocyanine derivatives are few,[8,9] and naphtho-pzs are, to the best of our knowledge, absent from the literature. The near-infrared (NIR) absorption/emission of these compounds, like related benzo-pzs,[10,11] makes them candidates for optical imaging applications[12,13] and we here report on their uptake by carcinoma cells. Elsewhere, we show that pz self-assembled monolayers (SAMs) provide a unique opportunity to study the factors that control the electron transport properties of electrode-adsorbed monolayers.[14,15]

The $H_2[pz(A_{4-n};C_n)]$ are synthesized by Linstead cross-macrocyclization[16] of isoindoline **3** with maleonitriles **4** or **5**, the latter having two chiral centers in the (*R*) configuration (Scheme 1); macrocycles with $n = 1$ (**6**, **8**), and $n =$ *trans*-2, (**7**, **9**) have been isolated and purified.[11,17]

The hydroxyl groups of commercially available dinitrile **1** were alkylated by nucleophilic substitution to form **2**; subsequent imidation to yield **3** was achieved in reductive Na^0/NH_3 conditions, suspended in ethylene glycol at 135 °C. Macrocyclization of **4** or **5** with **3** was carried out under the usual Linstead, magnesium ion templated conditions. The products $Mg[pz(A_{4-n};C_n)]$ were demetalated by reaction with trifluoroacetic acid to yield the free-base $H_2[pz(A_{4-n};C_n)]$, which were separated by chromatography to yield $H_2[pz(A_3;C)]$ (**6**, **8**), and *trans*-$H_2[pz(A_2;C_2)]$ (**7**, **9**) in up to 35% yield, along with minor amounts of $H_2[pz(A_4)]$.[11,18] The

(1) Bryant, G. C.; Cook, M. J.; Ryan, T. G.; Thorne, A. J. *J. Chem. Soc., Chem. Commun*. **1995**, 467–468.
(2) Piechocki, C.; Simon, J.; Skoulios, A.; Guillon, D.; Weber, P. *J. Am. Chem. Soc*. **1982**, *104*, 5245–5247.
(3) Diazgarcia, M. A.; Ledoux, I.; Duro, J. A.; Torres, T.; Agullolopez, F.; Zyss, J. *J. Phys. Chem*. **1994**, *98*, 8761–8764.
(4) Bonnett, R. *Chem. Soc. Rev*. **1995**, 19–33.
(5) Pandey, R. K.; Zheng, G. In *The Porphyrin Handbook*; Kadish, K. M., Smith, K. M., Guilard, R., Eds.; Academic Press: New York, 2000; Vol. 6, pp 157−227.
(6) Michel, S. L. J.; Baum, S.; Barrett, A. G. M.; Hoffman, B. M. *Prog. Inorg. Chem*. **2001**, *50*, 473–590.
(7) Fuchter, M. J.; Zhong, C.; Zong, H.; Hoffman, B. M.; Barrett, A. G. M. *Aust. J. Chem*. **2008**, *61*, 235–255.
(8) Michelsen, U.; Kliesch, H.; Schnurpfeil, G.; Sobbi, A. K.; Wohrle, D. *Photochem. Photobiol*. **1996**, *64*, 694–701.
(9) Schnurpfeil, G.; Sobbi, A. K.; Michelsen, U.; Wohrle, D. *Proc. SPIE−Int. Soc. Opt. Eng*. **1997**, *3191*, 299–308.
(10) Trivedi, E. R.; Harney, A. S.; Olive, M. B.; Podgorski, I.; Moin, K.; Sloane, B. F.; Barrett, A. G. M.; Meade, T. J.; Hoffman, B. M. *Proc. Natl. Acad. Sci. U.S.A*. **2010**, *107*, 1284−1288.
(11) Lee, S.; White, A. J. P.; Williams, D. J.; Barrett, A. G. M.; Hoffman, B. M. *J. Org. Chem*. **2001**, *66*, 461–465.
(12) Ntziachristos, V. *Annu. Rev. Biomed. Eng*. **2006**, *8*, 1–33.
(13) Sevick-Muraca, E. M.; Houston, J. P.; Gurfinkel, M. *Curr. Opin. Chem. Biol*. **2002**, *6*, 642–650.
(14) Vesper, B. J.; Salaita, K.; Zong, H.; Mirkin, C. A.; Barrett, A. G. M.; Hoffman, B. M. *J. Am. Chem. Soc*. **2004**, *126*, 16653–16658.
(15) Zong, H.; Sun, P.; Mirkin, C. A.; Barrett, A. G. M.; Hoffman, B. M. *J. Phys. Chem. B* **2009**, *113*, 14892–14903.
(16) Linstead, R. P.; Whalley, M. *J. Chem. Soc*. **1952**, 4839–4844.
(17) Bellec, N.; Montalban, A. G.; Williams, D. B. G.; Cook, A. S.; Anderson, M. E.; Feng, X.; Barrett, A. G. M.; Hoffman, B. M. *J. Org. Chem*. **2000**, *65*, 1774–1779.
(18) Trivedi, E. R.; Vesper, B. J.; Weitman, H.; Ehrenberg, B.; Radosevich, J. A.; Barrett, A. G. M.; Hoffman, B. M. *Photochem. Photobiol*. **2010**, In Press.

DOI: 10.1021/jo9026947 Published on Web 02/05/2010

SCHEME 1. Synthesis of Naphtho-pzs 6−9[a]

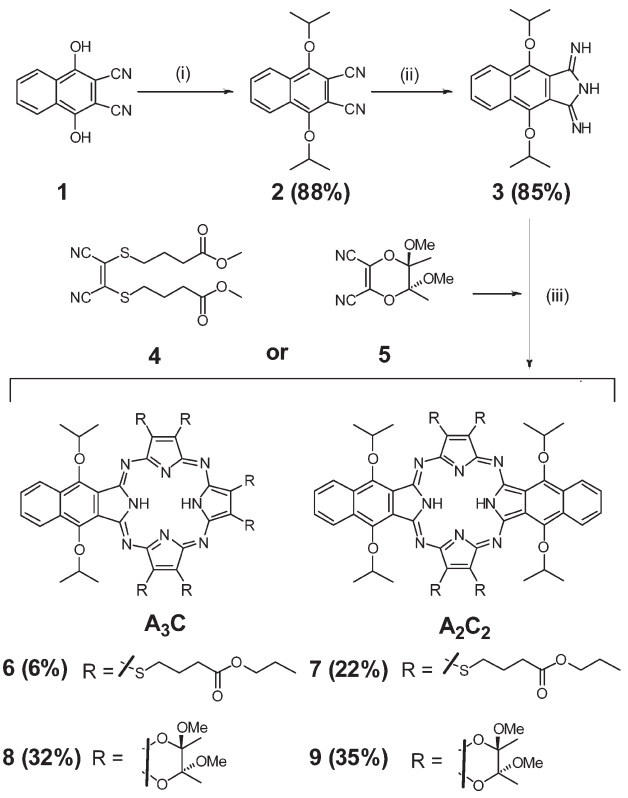

[a]Reagents and conditions: (i) iPr-Br, K_2CO_3/DMF, reflux, 24 h; (ii) NH_3/Na, ethylene glycol, 130 °C, 6 h; (iii) $Mg(OPr)_2$, 100 °C, 8 h.

two chiral centers of dinitrile **5** are retained in the final products, **8** and **9**. None of the *cis*-H_2[pz(A_2;C_2)] pigment was detected indicating that under these conditions, isoindoline **3** reacts preferentially with its cocyclization partners, to give the trans structure. The extent of which compounds are formed (n = 0, 1, or 2) varies with the ratio of the two cyclization partners. For example, due to the higher reactivity of maleonitriles than isoindolines under Linstead conditions, equimolar reaction of **4** or **5** with **3** yields large amounts of H_2[pz(A_4)] with very little H_2[pz(A_3;C)] (**6**, **8**), and no *trans*-H_2[pz(A_2;C_2)] (**7**, **10**) observed. Alternatively, slow addition of **4** or **5** into an excess of **3** under Linstead conditions has just the opposite effect with more *trans*-H_2[pz(A_2;C_2)] (**8**, **10**) produced, but the steric demand of **3** prevents any of the *cis*-H_2[pz(A_2;C_2)] and H_2[pz(A;C_3)] from being formed.

Black plate crystals of **7** were grown by slowly evaporating a saturated solution (CH_2Cl_2/MeOH) and their structure determined by X-ray diffraction analysis (Figure 1). Steric congestion at the periphery of related porphyrin and phthalocyanine systems causes the macrocycle core to be nonplanar,[19,20] but this effect is diminished in **7** by the $\pi-\pi$ stacking and orthogonality of bulky ester side chains. The unit cell contains a dimer in which pzs are aligned in parallel with 2.988(4) Å between planes (Figure 1), shorter than the typical naphthalocyanine intermolecular distances of ~3.3−5.0 Å.[21,22] The extended π-system afforded by this naphtho-pz core is expected to interact more strongly with Au surfaces than the related benzo-pzs, which are shown by angle-resolved XPS measurements to be lying down on the surface to form a SAM of thickness 3.9 Å.[23]

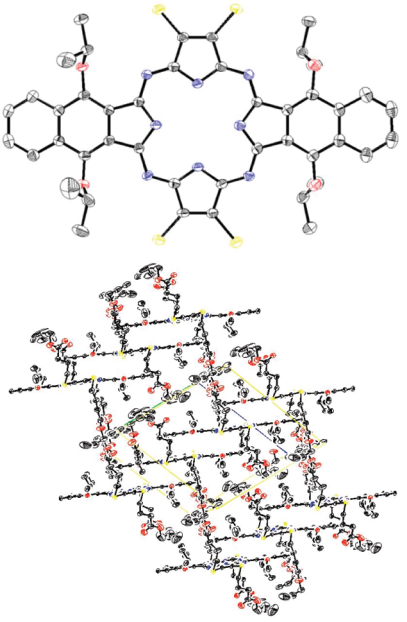

FIGURE 1. (Upper) X-ray crystal structure of *trans*-H_2[pz(A_2;C_2)] (**7**) with ester side chains and hydrogen atoms omitted for clarity. (Lower) Columnar stacks of **7** viewed along the *a*-axis.

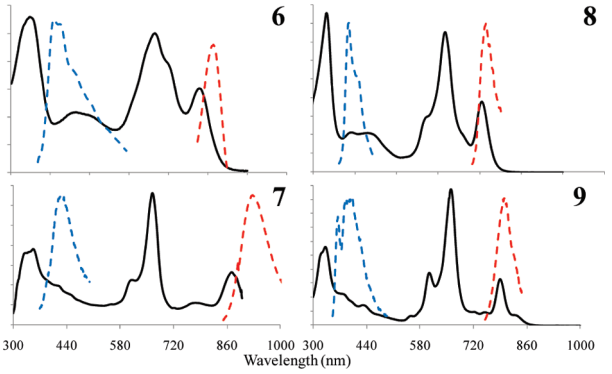

FIGURE 2. Absorption (black) and emission (S_2, blue; S_1, red) for H_2[pz(A_3;C)] (**6**, **8**) and *trans*-H_2[pz(A_2;C_2)] (**7**, **9**).

Heteroatom substituted H_2[pz(A_{4-n};C_n)] naphtho-pzs **6**−**9**, like the analogous H_2[pz(A_{4-n};B_n)] benzo-pzs,[24] display three absorption features (Figure 2): the Soret band ($\lambda < 400$ nm), the Q-band ($\lambda > 700$ nm), and a broad peak ($\lambda \approx 500$ nm) attributed to the n−π* transition of lone pair electrons on appended heteroatoms (S or O).[25] The choice of heteroatom

(19) Nurco, D. J.; Medforth, C. J.; Forsyth, T. P.; Olmstead, M. M.; Smith, K. M. *J. Am. Chem. Soc.* **1996**, *118*, 10918–10919.
(20) Chambrier, I.; Cook, M. J.; Wood, P. T. *J. Chem. Soc., Chem. Commun.* **2000**, 2133–2134.
(21) Morishige, K.; Araki, K. *J. Chem. Soc., Dalton* **1996**, 4303–4305.
(22) Pandian, R. P.; Dang, V.; Manoharan, P. T.; Zweier, J. L.; Kuppusamy, P. *J. Magn. Reson.* **2006**, *181*, 154–161.
(23) Sun, P.; Zong, H.; Salaita, K.; Ketter, J. B.; Barrett, A. G. M.; Hoffman, B. M.; Mirkin, C. A. *J. Phys. Chem. B* **2006**, *110*, 18151–18153.
(24) Forsyth, T. P.; Williams, D. B. G.; Montalban, A. G.; Stern, C. L.; Barrett, A. G. M.; Hoffman, B. M. *J. Org. Chem.* **1998**, *63*, 331–336.
(25) Kobayashi, N.; Konami, H. In *Phthalocyanines: Properties and Applications*; Leznoff, C. C., Lever, A. B. P., Eds.; VCH Publishers, Inc.: New York, 1996; Vol. 4, pp 343−404.

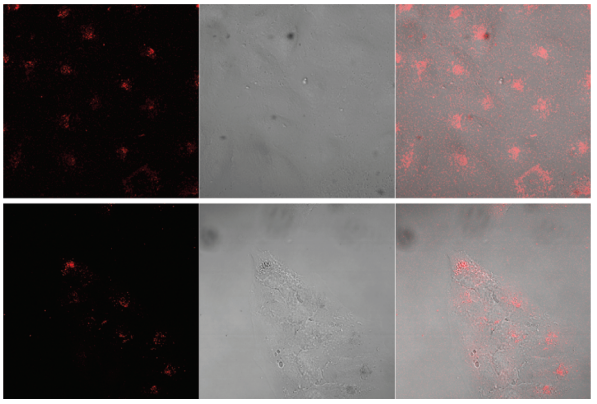

FIGURE 3. Confocal fluorescence microscopic images of A549 lung carcinoma cells treated with 50 μM pz **8** (upper) and **9** (lower): (left) long-wavelength emission; (middle) differential interference contrast image; and (right) overlay.

has a significant effect, as sulfur atoms red-shift the absorption bands by ~100 nm relative to their oxygen atom appended counterparts. In the case of 4-fold symmetric pzs, the Q-band appears as a single sharp peak. This symmetry is broken with the addition of "C" groups and the presence of internal pyrrole protons, splitting the Q-band. Although the major Q-band absorption is similar for the two types of pz heteroatom substituents (S or O), the Q-band splitting for the sulfide appended pzs is much larger, reaching as much as 3641 cm^{-1} for *trans*-H_2[pz(A_2;C_2)] (**7**). For H_2[pz(A_{4-n};C_n)], as *n* decreases the Q-band shifts to longer wavelengths and the n$-\pi^*$ transition diminishes as the number of appended heteroatoms decreases.

Dual-emission is observed for naphtho-pzs **6**−**9** from both the S_1 and S_2 excited singlet states (Figure 2). The *trans*-pzs **7** and **9** have the most intense emission of the series, making them excellent candidates as contrast agents for biomedical optical imaging applications.

To test the applicability of naphtho-pzs as optical contrast agents, A549 human lung carcinoma cells were treated with 50 μM **8** and **9** for 24 h and imaged via confocal fluorescence microscopy. Long-wavelength intracellular fluorescence from **8** and **9** is observed (Figure 3), appearing brighter than vehicle control images (see the Supporting Information). The observable intracellular fluorescence from such a naphtho-pz suggests utility as a standalone optical contrast agent or, with optimization of PDT action, as a theranostic tool that offers both early detection and treatment of cancer by a single agent.

Naphtho-pz derivatives **6**−**9**, which have been prepared in an analogous procedure to that of benzo-pzs, show major electronic absorptions shifted far into the NIR, demonstrating the synthetic tunability of optical properties for this pz system. Dual emission is observed from the first and second excited singlet states and is strongest for *trans*-H_2[pz(A_2;C_2)], **7** and **9**. The S_1 emission bands of **8** and **9** can be visualized in cell culture via confocal fluorescence microscopy confirming cellular uptake.

Experimental Section

1,4-Bis(1-methylethoxy)-2,3-naphthalenedicarbonitrile (2). 2-Bromopropane (30 mL) was added with vigorous stirring to a slurry of 1,4-dihydroxy-2,3-naphthalenedicarbonitrile (**1**) (15 g, 71 mmol) and K_2CO_3 (30 g, 217 mmol) in DMF (300 mL) and the resulting solution was heated at 60 °C for 48 h. The reaction mixture was poured into water (1 L) and vigorously stirred. The resulting white crystalline solid was collected by filtration and triturated with hot MeOH to yield **2** (18.4 g, 88%): mp 121−122 °C; IR (neat) ν_{max} 2985, 2218 cm^{-1}; ^{1}H NMR (500 MHz, $CDCl_3$) δ 1.49 (d, J = 6.1 Hz, 12H), 4.98 (hp, J = 6.1 Hz, 2H), 7.76 (q, J = 3.0 Hz, 2H), 8.25 (q, J = 3.0 Hz, 2H); ^{13}C NMR (125 MHz, $CDCl_3$) δ 22.9, 80.2, 100.7, 114.9, 124.2, 130.5, 131.5, 156.5; HRMS (ESI) (m/z) $[M + H]^+$ calcd for $C_{18}H_{19}N_2O_2$ 295.1447, found 295.1447.

4,7-Bis(1-methylethoxy)benzo[*f*]-1,3-diiminoisoindoline (3). Dinitrile **3** (19 g, 65 mmol) was suspended in ethylene glycol (400 mL) and the mixture was heated to 140 °C. After NH_3 (g) was bubbled through the solution for 30 min, freshly cut Na (0.7 g) was added, and NH_3 (g) was bubbled continuously through the solution for an additional 6 h. The solution was allowed to cool to room temperature and was poured into water (1.5 L). The yellow solid was collected by filtration, dried under vacuum, and purified by chromatography on silica (eluant MeOH:CH_2Cl_2 5:95; MeOH:CH_2Cl_2 8:92) to yield isoindoline **3** (17.1 g, 85%) as a pale yellow solid: mp 195−196 °C; IR (neat) ν_{max} 3440, 2970 cm^{-1}; ^{1}H NMR (500 MHz, $CDCl_3$) δ 1.45 (d, J = 6.0 Hz, 12H), 4.82 (hp, J = 6.0 Hz, 2H), 7.62 (q, J = 3.0 Hz, 2H), 8.18 (q, J = 3.0 Hz, 2H), 8.61 (br s, 3H); ^{13}C NMR (125 MHz, $CDCl_3$) δ 22.8, 78.7, 124.6, 127.8, 128.1, 132.4 147.0, 169.9; HRMS (ESI) (m/z) $[M + H]^+$ calcd for $C_{18}H_{22}N_3O_2$ 312.1075, found 312.1075.

[(4-Propyloxy-4-oxo-1-butyl)thio]naphthoporphyrazines 6 and 7. Mg turnings (0.1 g, 4.1 mmol) and I_2 (0.01 g) in *n*-PrOH (100 mL) were heated at reflux for 24 h under N_2 to prepare Mg(OPr)$_2$. Isoindoline **3** (2.48 g, 7.96 mmol) was added and the suspension was heated to reflux for 30 min, dinitrile **4** (0.68 g, 1.99 mmol) was added and the mixture was stirred at reflux for 8 h. The solution immediately turned a dark brown color and finally green-black. Solvent was removed under reduced pressure and the green-black residue was dissolved in CH_2Cl_2 (60 mL). TFA (3 mL) was added dropwise and the solution was stirred at room temperature for 30 min and diluted with CH_2Cl_2 (100 mL). The mixture was neutralized with aqueous $NaHCO_3$, washed with a large amount of water to remove salts, dried (Na_2SO_4), and rotary evaporated. During cyclization in *n*-propanol, the methyl ester was converted to the *n*-propyl ester by trans-esterification. The resulting residue was chromatographed on silica (eluant EtOAc:CH_2Cl_2 1:19) to yield pz **6** (54 mg, 5.5%) as a dark blue solid and pz **7** (307 mg, 22%) as a dark green solid, as well as trace amounts of the A_4 pz. The dyes eluted in the order **6** and **7**. The A_4 pz was characterized as previously reported.[11]

19,22-Bis(1-methylethoxy)-4,5,9,10,14,15-hexakis[(4-propyloxy-4-oxo-1-butyl)thio]-23*H*,25*H*-naphtho[*b*] porphyrazine (6). UV−vis (CH_2Cl_2) λ_{max} (log ε) 352 (4.56), 665 (4.54), 781 (4.33) nm; ^{1}H NMR (500 MHz, $CDCl_3$) δ 0.76 (t, J = 7.3 Hz, 6H), 0.85 (t, J = 7.3 Hz, 6H), 0.88 (t, J = 7.3 Hz, 6H), 1.46 (q, J = 7.3 Hz, 4H), 1.56 (q, J = 7.3 Hz, 4H), 1.59 (q, J = 7.3 Hz, 4H), 11.66 (d, J = 6.1 Hz, 12H), 2.02 (tt, J = 7.0 Hz, J = 7.3 Hz, 4H), 2.16 (tt, J = 7.0 Hz, J = 7.3 Hz, 4H), 2.27 (tt, J = 7.0 Hz, J = 7.3 Hz, 4H), 2.60 (t, J = 7.3 Hz, 4H), 2.66 (t, J = 7.3 Hz, 4H), 2.72 (t, J = 7.0 Hz, 4H), 3.86 (t, J = 7.0 Hz, 4H), 3.92−4.00 (t, J = 7.3 Hz, 12H), 4.00 (t, J = 7.0 Hz, 4H), 4.32 (t, J = 7.0 Hz, 4H), 6.24 (hp, J = 6.1 Hz, 2H), 7.87 (q, J = 3.1 Hz, 2H), 8.83 (q, J = 3.1 Hz, 2H); ^{13}C NMR (125 MHz, $CDCl_3$) δ 10.5, 10.6, 22.1, 22.2, 23.4, 25.6, 25.8, 26.0, 33.1, 33.3, 33.4, 34.4, 34.7, 34.9, 66.2, 66.26, 66.33, 125.8, 128.4, 133.7, 135.1, 139.8, 143.0, 149.3, 173.25, 173.30, 173.36; HRMS (ESI) (m/z) $[M + H]^+$ calcd for $C_{72}H_{99}N_8O_{14}S_6$ 1491.5611, found 1491.5611.

1,4,13,16-Tetrakis(1-methylethoxy)-8,9,20,21-tetra[(4-propyloxy-4-oxo-1-butyl)thio]-25*H*,27*H*-dinaphtho[*b*,*l*] porphyrazine (7). UV−vis (CH_2Cl_2) λ_{max} (log ε) 348 (4.62), 609 (sh), 663

(4.91), 875 (4.53) nm; ^{1}H NMR (500 MHz, $CDCl_3$) δ 0.76 (t, J = 7.3 Hz, 12H), 1.46 (m, 8H), 1.67 (d, J = 6.1 Hz, 24H), 2.04 (tt, J = 7.2 Hz, J = 6.9 Hz, 8H), 2.59 (t, J = 7.2 Hz, 8H), 3.86 (t, J = 6.8 Hz, 8H), 4.09 (t, J = 6.9 Hz, 8H), 6.14 (hp, J = 6.1 Hz, 4H), 7.82 (m, 4H), 8.81 (m, 4H); ^{13}C NMR (125 MHz, $CDCl_3$) δ 10.5, 22.1, 23.4, 25.8, 33.2, 35.1, 66.1, 76.7, 125.5, 127.0, 127.6, 133.1, 137.6, 144.3, 148.0, 160.2, 173.3; HRMS (ESI) (m/z) $[M + H]^+$ calcd for $C_{72}H_{91}N_8O_{12}S_4$ 1387.564, found 1387.564.

[(2*R*,3*R*)-2,3-Dimethoxy-2,3-dimethyl-1,4-diox-2-ene]naphthoporphyrazines 8 and 9. Pzs **8** and **9** were prepared from **3** (0.710 g, 2.28 mmol) and **5** (0.092 g, 0.41 mmol) by a procedure identical with that for the preparation of **6** and **7**, using Mg (0.02 g, 0.82 mmol) in *n*-PrOH (50 mL). The resulting solid was chromatographed on silica (eluant EtOAc:hexanes 1:3) to yield pz **8** (46 mg, 35%) as a dark blue solid and pz **9** (69 mg, 32%) as a dark green solid, as well as trace amounts of the A_4 pz. The dyes eluted in the order **8** and **9**. The A_4 pz was characterized as previously reported.[18]

18,25-Bis(1-methylethoxy)tris[1,4-dioxino[*g*,*l*,*q*]-(2*R*,3*R*)-2,3-dimethoxy-2,3-dimethyl]-29*H*,31*H*-naphtho[*b*]porphyrazine (8). UV−vis (CH_2Cl_2) λ_{max} (log ε) 333 (4.23), 618 (4.18), 707 (3.87); ^{1}H NMR (500 MHz, $CDCl_3$) δ 1.77 (d, J = 6.0 Hz, 6H), 1.83 (d, J = 6.0 Hz, 6H), 1.98 (s, 6H), 2.01 (s, 6H), 2.04 (s, 6H), 3.45 (s, 6H), 3.47 (s, 6H), 6.25 (hp, J = 6.0 Hz, 2H), 7.73 (m, 2H), 8.81 (m, 2H); ^{13}C NMR (125 MHz, $CDCl_3$) δ 18.06, 18.09, 18.24, 23.38, 23.51, 50.08, 50.14, 50.3, 78.1, 102.0, 102.3, 102.5, 125.4, 126.9, 127.5, 133.1, 134.1, 135.8, 136.1, 137.0, 138.4, 148.5, 149.7, 160.2; HRMS (ESI) (m/z) $[M + H]^+$ calcd for $C_{48}H_{57}N_8O_{14}$ 969.399, found 969.400.

8,15,26,33-Tetrakis(1-methylethoxy)di[1,4-dioxino[*g*,*q*]-(2*R*,3*R*)-2,3-dimethoxy-2,3-dimethyl]-37*H*,39*H*-dinaphtho[*b*,*l*]porphyrazine (9). UV−vis (CH_2Cl_2) λ_{max} (log ε) 333 (4.42), 608 (4.24), 663 (4.61), 789 (4.08); ^{1}H NMR (500 MHz, $CDCl_3$) δ 1.75 (d, J = 5.9 Hz, 12H), 1.86 (d, J = 5.9 Hz, 12H), 2.03 (s, 12H), 3.53 (s, 12H), 6.21 (hp, J = 5.9 Hz, 4H), 7.71 (m, 4H), 8.80 (m, 4H); ^{13}C NMR (125 MHz, $CDCl_3$) δ 18.0, 23.4, 23.5, 50.1, 78.0, 102.4, 125.3, 126.9, 127.1, 132.6, 134.2, 136.0, 147.9, 158.3; HRMS (ESI) (m/z) $[M + H]^+$ calcd for $C_{56}H_{63}N_8O_{12}$ 1039.457, found 1039.456.

Acknowledgment. This work was supported primarily by the Nanoscale Science and Engineering Initiative of the National Science Foundation under NSF Award No. EEC-0647560. This work has also been supported by the NSF Award No. CHE0500796 and the Penny Severns Breast, Cervical, and Ovarian Cancer Research Fund.

Supporting Information Available: Experimental procedures, ^{1}H and ^{13}C NMR spectra for new compounds, single-crystal X-ray data for **7** (CIF), and negative controls for fluorescence imaging assays. This material is available free of charge via the Internet at http://pubs.acs.org.